Odd-even width effect on persistent current in zigzag hexagonal graphene rings

ARTICLE *in* NANOSCALE · DECEMBER 2009

Impact Factor: 7.39 · DOI: 10.1039/b9nr00044e · Source: PubMed

3 AUTHORS, INCLUDING:

Mingming Ma
Huazhong University of Science and Techn…

Ningying Xu
Zhejiang University

Odd–even width effect on persistent current in zigzag hexagonal graphene rings

M. M. Ma, J. W. Ding* and N. Xu

Received 29th April 2009, Accepted 24th August 2009
First published as an Advance Article on the web 29th September 2009
DOI: 10.1039/b9nr00044e

The electronic structure and thus the persistent current of zigzag hexagonal graphene rings are investigated within the tight-binding formalism. The flux-dependent energy spectrum is grouped into bands with six levels per band due to inter-valley scattering at the corners of the ring. It is found that the degeneracy at the Fermi level is determined by the even or odd quality of the ring width N. The sample ring becomes metallic at odd N but semiconducting at even N, showing up a strange odd–even width effect. In metallic rings, the persistent current within a flux period is linearly changed with magnetic flux ϕ, while it is a sinusoidal periodical function of ϕ in semiconducting rings. In addition, with increasing N, the persistent current exponentially decreases (increases) at odd (even) N, but finally falls into the consistence with each other at enough large N, showing that the odd–even effect may be experimentally observable only in narrow rings.

Graphene, a single atomic layer of graphite adhered from natural graphite,[1,2] has been attracting much intensive research in both theory and experiment due to its peculiar electronic and magnetic transport properties.[3–7] Indeed, a mass of graphene-based structures have been fabricated due to experimental and theoretical breakthroughs over the past decade, which may be used as building blocks for nanometre-scale devices. More recently, it was reported that graphene can be cut or patterned into well-defined geometric structures by different techniques,[8–14] further opening the door to the fabrication of graphene-based nanodevices. For instance, various graphene-based functional elements and components have been obtained experimentally such as quantum dots,[9–11] field-effect transistors,[12,13] integrated graphene circuits[14] *etc.* Especially, a new style of ring-shaped graphene was fabricated with inner and outer radii of about 350 nm and 500 nm,[15] which may be one of the most novel building blocks for future electromagnetic nanodevices. Due to their similarity to mesoscopic rings, the unusual electronic properties of graphene rings have attracted great interest in theory,[16,17] indicating they are a useful candidate for probing both quantum coherence and dephasing rates of systems. Of special interest is the persistent current[18–20] in such a two-dimensional (2D) ring-shaped device, induced by magnetic flux, ϕ, threaded through the centre of the ring.

For graphene-based structures, the electronic properties of graphene nanoribbons (GNRs), carbon nanotubes (CNTs), and toroidal carbon nanotubes (TCNs) have been well studied, and are dependent upon their geometries. It is well known that all zigzag GNRs are metallic regardless of width,[21,22] while armchair GNRs can be either metallic or insulating depending on their widths.[22–25] As for armchair CNTs and TCNs, they have the same armchair-type cross-section as in zigzag GNRs.

Department of Physics & Institute for Nanophysics and Rare-earth Luminescence, Xiangtan University, Xiangtan, 411105 Hunan, China. E-mail: jwding@xtu.edu.cn

Not considering the curvature, all armchair CNTs and TCNs are expected to be metallic,[26–29] similar to zigzag GNRs. For zigzag hexagonal graphene rings (HGRs), it is interesting to explore whether similar characteristics come into existence and how the metallicity depends on its geometry. The study of zigzag HGRs would be very helpful to obtain universal laws of quantum-size effects on electronic transport in graphene-based structures.

For various-shaped HGRs, recently, the inner- and outer-edge states have been obtained, which depend on the edge symmetries and the corner structures.[30] For zigzag HGRs, especially, the charge density is spread out on the two opposite edges, indicating the coupling of states localized at two opposite edges. Therefore, one may expect that the effects of ring size and edge-state coupling are very important for determining the electronic structures and thus the persistent currents in zigzag HGRs, which should be further explored.

By developing the supercell method,[31] we present a detailed investigation on the electronic structures, and thus the persistent currents of zigzag HGRs. The results show that the flux-dependent energy spectrum is grouped into bands with six levels per band, due to the inter-valley scattering at the corners of the ring. More interestingly, it is found that the parity of the ring width N determines the degeneracy at the Fermi level ($E_F = 0$) and thus the metallicity of the samples, which are metallic at odd N but semiconducting at even N, showing up a strange odd–even width effect. For a metallic ring, the persistent current is a linearly periodical function of magnetic flux, ϕ, while it is a sinusoidal periodical function of ϕ for semiconducting rings. In addition, with increasing N, the persistent current decreases (increases) at odd (even) N, but finally falls into consistence with each other at enough large N. This indicates that the odd–even width effect may be experimentally observable only in narrow rings.

A HGR of zigzag edge is shown in Fig. 1(a) consisting of six arms with l the lattice spacing, the inner ring radius r is given in

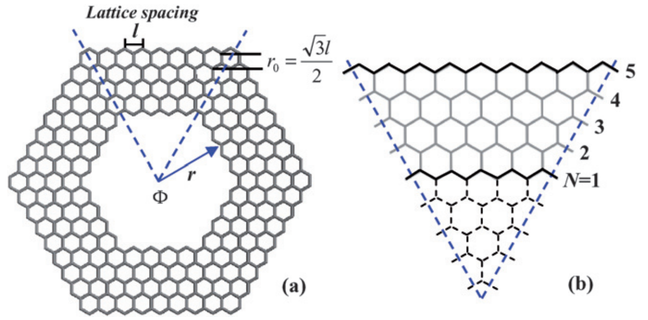

Fig. 1 (a) A zigzag HGR of ring width $N = 5$ and inner ring radius $r = 4r_0$ with l the lattice spacing and $r_0 = \sqrt{3}l/2$. Magnetic flux, ϕ, passes through the hole. (b) Schematic illustration of one arm in the ring, of which the dashed hexagons in the centre are cut out.

units of r_0, and $r = 4r_0$ with $r_0 = \sqrt{3}l/2$. The geometry of one arm is schematized for width $W = Nr_0$ in Fig. 1(b), with $N = 5$ the number of zigzag carbon chains. We use the single-orbital nearest-neighbor tight-binding model for the finite-size HGR, which has been successfully applied to the study of GNRs,[22–25] CNTs[26,27] and other carbon-related materials.[28,29] In the present model, the magnetic field is limited to the central region of the ring. The Hamiltonian, neglecting electron–electron interactions, is given by

$$H = \sum_i \varepsilon_i |i\rangle\langle i| + \sum_{i,j} \tau_{i,j} |i\rangle\langle j| \tag{1}$$

where i and j label the nearest sites on a honeycomb lattice. In a perfect HGR, the on-site energies are taken as $\varepsilon_i = 0$. The hopping integral elements $\tau_{i,j} = -\tau \exp[(i2e/h)\int_i^j d\vec{r}\cdot\vec{A}]$ with $\tau = 2.9$ eV the hopping integral constant, and $\vec{A}$ is the vector potential. The electronic spectrum can be obtained by the supercell method recently developed by Liu and Ding.[31] In terms of the rotational symmetry of six-fold, the effective Hamiltonian of a supercell is given by

$$H_{\text{eff}} = H_0 + e^{i\beta}H_1 + e^{-i\beta}H_1^{+} \tag{2}$$

where H_0 and H_1 refer to the Hamiltonian matrix in the supercell and the coupling matrix between the two neighboring supercells, respectively. Here $\beta = j \times 2\pi/P$, ($j = 1, 2, \ldots, P$) is the phase difference between the wave functions of two neighboring supercells, where $P = 6$ is the number of the supercells contained in the HGR. For a given β, the eigenlevels can be obtained by diagonalizing the matrix H_{eff}. This simplified calculation is a reasonable and efficient method for such similar complex system with rotational symmetry.

At zero temperature, the total persistent current of system is given by

$$I_{\text{pc}} = -\partial E/\partial\Phi = -\sum_n \partial E_n/\partial\Phi = -\frac{1}{\Phi_0}\sum_n \partial E_n/\partial\phi \tag{3}$$

where $\phi = \Phi/\Phi_0$ is the dimensionless magnetic flux with $\Phi_0 = h/e$ the flux quantum. E_n is the energy of the system, and n labels the corresponding eigenlevels. The current is a periodic function of ϕ with fundamental period Φ_0. Usually, one is interested in the typical current,[20] which is defined as the square-root of the flux average of the square of the persistent currents, given by

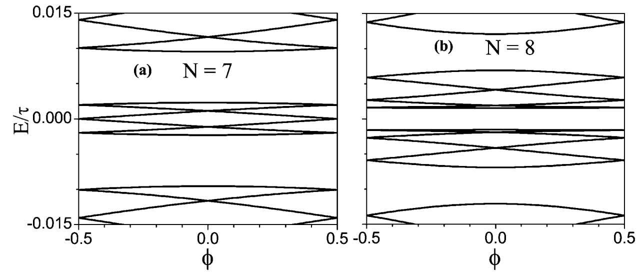

Fig. 2 Energy spectra of zigzag HGRs as a function of magnetic flux for the sizes $r = 13r_0$, (a) $N = 7$ and (b) $N = 8$.

$$I_{\text{typ}} = \sqrt{\langle I_{\text{pc}}{}^2 \rangle_\Phi}\ . \tag{4}$$

In our calculations, the site energies ε_i and energy E are given in units of τ, and thus the persistent currents in units of τ/Φ_0. As typical examples, Fig. 2 shows the energy spectrum near the Fermi level of the zigzag HGRs of $N = 7$ (a) and $N = 8$ (b). Both rings have the same inner ring radius of $r = 13r_0$. From Fig. 2, it is seen that the flux-dependent energy spectrum is grouped into bands, with six levels per band in both cases, which may be due to the high-symmetry structure of HGRs. For each site in such a ring, there exist other five equivalent sites, due to the six-fold rotational symmetry. Because of the long distance between them, the six sites are weakly coupled to each other by other sites. This may lead to a six-level group of bands. For the sites located in a supercell, however, there exists not only strong interactions with the neighboring sites but also the inter-valley scattering at the corners,[16] which would result in the presence of inter-band gaps. From Fig. 2, especially, it is found that the energy spectrum strongly depends on the odd or even quality of the ring width N. In the case of $N = 7$ in Fig. 2(a), the highest occupied state (HOS) and the lowest unoccupied state (LUS) are degenerate at $\Phi = \pm 0.5\Phi_0$, showing the sample ring to be metallic. In Fig. 2(b) with $N = 8$, a narrow energy gap appears at $\Phi = \pm 0.5\Phi_0$, indicating the sample ring to be a narrow-gap semiconductor. Further calculations have been done for other zigzag HGRs of both odd and even N. It follows that zigzag HGRs are metallic at odd N and semiconducting at even N. The result can be understood by the following consideration.

From Fig. 1(b), it is clearly seen that for a zigzag HGR, the number of atoms within each zigzag chain in one arm must be odd, irrespective of inner radius r. Thus, the number of atoms N_1 in one arm must be odd (even) only if N is odd (even). Due to spin degeneration and the rotational symmetry of six-fold, further, the highest occupied band is obtained to be $N_1/2$. This means that for an odd N (or N_1), the Fermi level is located at the centre of the $(N_1 + 1)/2$ band, while it falls into the gap between $N_1/2$ and $N_1/2 + 1$ at even N (or N_1). Therefore, the even or odd quality of the ring width N determines completely the degeneracy at the Fermi level and thus the metallicity of a zigzag HGR. The result is different from the observation of odd–even effect in the conductance of zigzag GNRs under gate potentials,[32–34] which is attributed to the symmetry and asymmetry of the zigzag chains of GNRs.

From the energy spectrum of the studied samples, in Fig. 3, we calculate the persistent currents (I_{pc}) of the zigzag HGRs as a function of magnetic flux, ϕ, for metallic rings with odd N (a) and semiconducting rings with even N (b). For the metallic ring

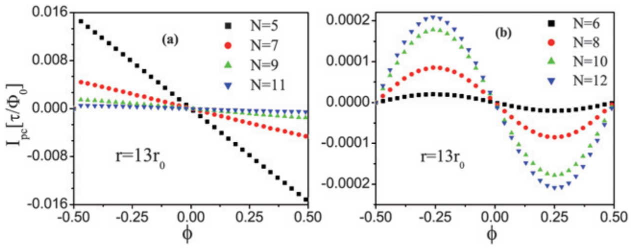

Fig. 3 Persistent currents of zigzag HGRs as a function of magnetic flux for (a) odd N, and (b) even N.

in Fig. 3(a), it is shown that the flux-dependent I_{pc} within a period flux changes linearly with ϕ. A jump of I_{pc} is observed at $\Phi = \pm 0.5\Phi_0$, corresponding to the level degeneracy at $\Phi = \pm 0.5\Phi_0$ as shown in Fig. 2(a), similar to that of TCNs of metallic-type I.[28,29] For semiconducting rings, it is seen from Fig. 3(b) that at a given inner radius r, the persistent current may decline by 2–3 orders of magnitude at small N, compared with the metallic ring. This may be due to the energy gap and an almost zero slope of energy curves near the Fermi level in the semiconducting ring, as shown in Fig. 2(b). Also, its behavior of flux-dependent I_{pc} is a smooth sinusoidal periodical function of ϕ, different from the metallic HGR. From Figs. 3 (a) and (b), in addition, it is seen that with increasing N, I_{pc} decreases at odd N but increases at even N, further showing up a strange odd–even width effect.

To explore the quantum-size effect on persistent current, in Fig. 4(a), we plot the logarithm of the typical currents (I_{typ}) in zigzag HGRs as a function of the inner ring radius r. From Fig. 4(a), it is seen that for both metallic and semiconducting rings, the overall I_{typ} decreases with increasing r, as expected in the previous theory of mesoscopic metallic rings.[20] From a more careful analysis, it is found that the data of I_{typ} *vs.* r are well fitted to $I_{typ} \sim \exp(-\kappa r/r_0)$. The decay exponent κ is obtained to be $\kappa = 0.4937$, 0.5616, and 0.6450 at $N = 5$, 7, and 9 respectively, while $\kappa = 1.3168$, 0.9956, and 0.8223 at $N = 4$, 6, and 8 respectively. This means that the typical currents also depend strongly on ring width N, κ decreasing (increasing) with N in metallic (semiconducting) rings, different from the previous results.[19,20]

In Fig. 4(b), we further show the logarithm of I_{typ} as a function of the ring width N. In the case of metallic rings (odd N), it is seen from Fig. 4(b) that with increasing N, I_{typ} firstly decreases exponentially at small N but becomes invariable at larger N. For semiconducting rings (even N), however, I_{typ} firstly increases exponentially with N, in spite of a constant I_{typ} at larger N. At a given inner ring radius r, especially, I_{typ} at two neighboring odd and even N falls finally into consistency at enough large N. Such changes in I_{typ} can be understood from the calculated energy spectra, of which the slopes of energy curves and the energy gaps change with N. For a large N, in fact, the wide ring can be regarded as a graphene sheet with vacancies in the presence of a perpendicular magnetic field,[35] in which the odd–even effect would disappear. Therefore, the odd–even width effect should be experimentally observable in narrow zigzag HGRs.

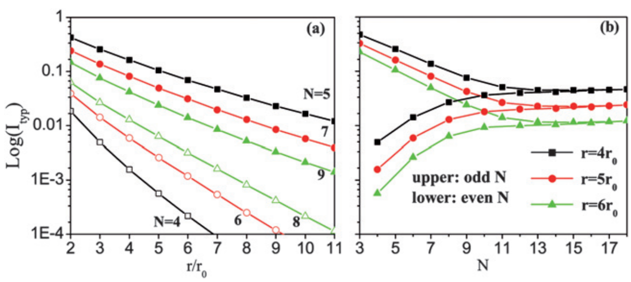

Fig. 4 Typical currents, I_{typ}, of zigzag HGRs as a function of (a) the inner ring radius r and (b) ring width N.

In conclusion, a detailed investigation is presented for the electronic structure and the persistent currents in zigzag HGRs by developing a supercell method within the single-orbital nearest-neighbor tight-binding model. The results show that the energy spectrum is grouped into bands with six levels per band, due to the inter-valley scattering at the corners of the ring. Interestingly, it is found that the parity of the ring width N determines the degeneracy at the Fermi level and thus the metallicity of the samples. It is shown that a sample ring of width N is metallic at odd N but semiconducting at even N, showing up a strange odd–even width effect. For metallic rings, the persistent current is a linearly periodical function of magnetic flux, ϕ, while it is a sinusoidal periodical function of ϕ for semiconducting rings. With increasing N, in addition, the persistent current exponentially decreases (increases) at odd (even) N and falls finally into consistency at large enough N, showing the strange odd–even width effect existing only in narrow rings. The results may be very helpful for the design and application of HGR-based nanodevices.

Acknowledgements

This work was supported by the National Natural Science Foundation of China (No. 10674113), the Program for New Century Excellent Talents in University (NCET-06-0707), and the Foundation for the Author of National Excellent Doctoral Dissertation of China (Grant No. 200726).

References

1 K. S. Novoselov, A. K. Geim, S. V. Morozov, D. Jiang, Y. Zhang, S. V. Dubonos, I. V. Grigorieva and A. A. Firsov, *Science*, 2004, **306**, 666–669.
2 K. S. Novoselov, A. K. Geim, S. V. Morozov, D. Jiang, M. I. Katsnelson, I. V. Grigorieva, S. V. Dubonos and A. A. Firsov, *Nature*, 2005, **438**, 197–200.
3 E. McCann, K. Kechedzhi, V. I. Falko, H. Suzuura, T. Ando and B. L. Altshuler, *Phys. Rev. Lett.*, 2006, **97**, 146805–146808.
4 S. V. Morozov, K. S. Novoselov, M. I. Katsnelson, F. Schedin, L. A. Ponomarenko, D. Jiang and A. K. Geim, *Phys. Rev. Lett.*, 2006, **97**, 016801–016804.
5 N. Xu and J. W. Ding, *J. Phys.: Condens. Matter*, 2008, **20**, 485213–485217.
6 Y. B. Zhang, Y. W. Tan, H. L. Stormer and P. Kim, *Nature*, 2005, **438**, 201–204.
7 T. Ohta, A. Bostwick, T. Seyller, K. Horn and E. Rotenberg, *Science*, 2006, **313**, 951–954.
8 C. Berger, Z. Song, X. Li, X. Wu, N. Brown, C. Naud, D. Mayou, T. Li, J. Hass, A. N. Marchenkov, E. H. Conrad, P. N. First and W. A. Heer, *Science*, 2006, **312**, 1191–1196.
9 K. S. Novoselov, Z. Jiang, Y. Zhang, S. V. Morozo, H. L. Stormer, U. Zeitler, J. C. Maan, G. S. Boebinger, P. Kim and A. K. Geim, *Science*, 2007, **315**, 1379–1379.
10 L. A. Ponomarenko, F. Schedin, M. I. Katsnelson, R. Yang, E. W. Hill, K. S. Novolevov and A. K. Geim, *Science*, 2008, **320**, 356–358.

11 S. Schnez, F. Molitor, C. Stampfer, J. Güttinger, I. Shorubalko, T. Ihn and K. Ensslin, *Appl. Phys. Lett.*, 2009, **94**, 012107–012109.
12 B. Obradovic, R. Kotlyar, F. Heinz, P. Matagne, T. Rakshit, M. D. Giles, M. A. Stettler and D. E. Nikonov, *Appl. Phys. Lett.*, 2006, **88**, 142102–142104.
13 T. J. Echtermeyer, M. C. Lemme, J. Bolten, M. Baus, M. Ramsteiner and H. Kurz, *Eur. Phys. J. Spec. Top.*, 2007, **148**, 19–26.
14 D. A. Areshkin and C. T. White, *Nano Lett.*, 2007, **7**, 3253–3259.
15 S. Russo, J. B. Oostinga, D. Wehenkel, H. B. Heersche, S. S. Sobhani, L. M. K. Vandersypen and A. F. Morpurgo, *Phys. Rev. B: Condens. Matter Mater. Phys.*, 2008, **77**, 085413–085417.
16 P. Recher, B. Trauzettel, A. Rycerz, Y. M. Blanter, C. W. J. Beenakker and A. F. Morpurgo, *Phys. Rev. B: Condens. Matter Mater. Phys.*, 2007, **76**, 235404–235408.
17 A. Rycerz, *Acta Physica Polonica A*, 2009, **115**, 322–325.
18 M. Büttiker, Y. Imry and R. Landauer, *Phys. Lett. A*, 1983, **96**, 365–367.
19 H. F. Cheung, Y. Gefen, E. K. Riedel and W. H. Shih, *Phys. Rev. B: Condens. Matter Mater. Phys.*, 1988, **37**, 6050–6062.
20 E. Louis, J. A. Verges and G. Chiappe, *Phys. Rev. B: Condens. Matter Mater. Phys.*, 1998, **58**, 6912–6919.
21 M. Ezawa, *Phys. Rev. B: Condens. Matter Mater. Phys.*, 2006, **73**, 045432–045439.
22 K. Nakada, M. Fujita, G. Dresselhaus and M. S. Dresslhaus, *Phys. Rev. B: Condens. Matter Mater. Phys.*, 1996, **54**, 17954–17961.
23 K. Wakabayashi, M. Fujita, H. Ajiki and M. Sigrist, *Phys. Rev. B: Condens. Matter Mater. Phys.*, 1999, **59**, 8271–8282.
24 Y. W. Son, M. L. Cohen and S. G. Louie, *Nature*, 2006, **444**, 347–349.
25 H. X. Zheng, Z. F. Wang, T. Luo, Q. W. Shi and J. Chen, *Phys. Rev. B: Condens. Matter Mater. Phys.*, 2007, **75**, 165414–165419.
26 J. W. Mintmire, B. I. Dunlap and C. T. White, *Phys. Rev. Lett.*, 1992, **68**, 631–634.
27 R. Saito, M. Fujita, G. Dresselhaus and M. S. Dresselhaus, *Phys. Rev. B: Condens. Matter Mater. Phys.*, 1992, **46**, 1804–1811.
28 M. F. Lin and D. S. Chuu, *Phys. Rev. B: Condens. Matter Mater. Phys.*, 1998, **57**, 6731–6737.
29 S. Latil, S. Roche and A. Rubio, *Phys. Rev. B: Condens. Matter Mater. Phys.*, 2003, **67**, 165420–165428.
30 D. A. Bahamon, A. L. C. Pereira and P. A. Schulz, *Phys. Rev. B: Condens. Matter Mater. Phys.*, 2009, **79**, 125414–125420.
31 C. P. Liu and J. W. Ding, *J. Phys.: Condens. Matter*, 2006, **18**, 4077–4084.
32 A. R. Akhmerov, J. H. Bardarson, A. Rycerz and C. W. J. Beenakker, *Phys. Rev. B: Condens. Matter Mater. Phys.*, 2008, **77**, 205416–205420.
33 A. Cresti, G. Grosso and G. P. Parravicini, *Phys. Rev. B: Condens. Matter Mater. Phys.*, 2008, **77**, 233402–233405.
34 Z. Li, H. Qian, J. Wu, B. L. Gu and W. Duan, *Phys. Rev. Lett.*, 2008, **100**, 206802–206805.
35 A. L. C. Pereira and P. A. Schulz, *Phys. Rev. B: Condens. Matter Mater. Phys.*, 2008, **78**, 125402–125406.

